Experiments in Fluids 10, 77–86 (1990)

Experiments in Fluids



# Interpretation of cyclic flow variations in motored internal combustion engines

**A. C. Enotiadis, C. Vafidis** and **J. H. Whitelaw**

Imperial College of Science, Technology and Medicine, Mechanical Engineering Dept., Fluids Section, Exhibition Road, London SW7 2BX, United Kingdom

**Abstract.** Cyclic variations and turbulence characterisation are considered in the context of in-cylinder flows. Three methods of data analysis, namely ensemble averaging, high pass filtering and cycle-by-cycle smoothing, are applied to velocity data obtained by laser Doppler velocimetry in a model axisymmetric and a realistic engine configuration. The interpretation of the results is supported by similar analysis of a steady-state simulation of in-cylinder flow with emphasis on the discrimination between random and deterministic flow variations. The results suggest that it is not always possible to identify cyclic variations as deterministic processes and that turbulence estimates based on filtering techniques may be misleading. The differences in the estimates of mean values are, however, small.

## 1 Introduction

It is well known that internal combustion engines are subject to variations of cylinder pressure from one cycle to another, which may impair performance. Similar phenomena can occur in all forms of rotating machinery and can be associated with fluid-dynamic, scalar-transport and combustion processes. It is generally appreciated that the combustion process in internal combustion engines requires the presence of an appropriately formed fuel-air mixture at the time of ignition and that cyclic variations of the intermittent combustion process can occur when the initial conditions prior to ignition are not repeatable. The method of ignition affects these variations but their existence can stem from poor mixing of fuel and air or from low-frequency variations of the in-cylinder turbulent flow field. These fluid mechanical variations emphasise the longer velocity scales, rather than the smaller scales essential for combustion and flame propagation, and can transport fuel away from the ignition site for periods of time large enough to affect performance.

The nature of cyclic variations has been considered in a number of papers, e.g. those of Winsor and Patterson (1974), Rask (1981), Liou and Santavicca (1983, 1985), Witze et al. (1984), Witze and Martin (1984), Catania and Mittica (1985), Fansler and French (1988), Glover (1986) and Daily (1988). The more recent papers are concerned largely with sampling and interpretation of cycle-resolved velocity information from in-cylinder flows, the importance of which is evident in the large differences in averaged values discussed, e.g., by Hall et al. (1986). Thus, it is desirable to correctly measure and analyse information from engines so as to understand the nature of cyclic variations and, where necessary, to remove them. This paper is concerned with velocity information from non-combusting engine flows and the conclusions have implications for cyclic variations in all forms of rotating machinery. It is important to appreciate that, although the emphasis of this paper is on the interpretation of velocity characteristics in terms of random and deterministic fluctuations, the practical requirement is to minimise the latter. It may be that cycle-by-cycle variations in velocity can be rendered negligible in many cases, so that analyses of the type considered here become unnecessary.

The present measurements and analysis follow from the earlier investigations of Vafidis (1984) and Arcoumanis et al. (1987) which observed the existence of swirl centre precession in model-engine arrangements and showed that the precession frequency scaled with engine speed and its amplitude diminished with radial distance from the centre of rotation. It was apparent that the origins of this phenomenon lay in the flow recirculation region downstream of the intake valve and that its magnitude depended on its confinement as well as the swirl level. This swirl centre precession constitutes a source of ordered periodic motion which may be contrasted with, but not always separated from, random turbulent fluctuations. In engine practice, it can give rise to cyclic variations in air-fuel mixture motion with ordered preference of large scales and consequent variations in the ignition process. In the present experiments, the precession of the swirl centre provides the superposition of an ordered periodic motion, of which we have some knowledge, upon the random turbulent fluctuations associated with the intake and compression strokes of an engine. The resulting velocity characteristics are measured here by laser velocimetry and the cycle-resolved velocity traces are examined to determine the effect of this cyclic variation on ensemble averages of moments of the axial and circumferential components. Previous attempts to separate random and ordered fluctuations

have made use of high-pass filters of one form or another and velocity autocorrelation analysis and the consequences of these approaches are examined.

The following section describes the experimental arrangements, together with the instrumentation used to obtain the cycle-resolved velocity information. The third section provides a brief description of averaging procedures, including those of Rask (1981) and Liou and Santavicca (1983, 1985). The results of the experiments and analysis are presented and discussed in the fourth section and the paper ends with a summary of the more important conclusions.

## 2 Flow configurations and instrumentation

Laser Doppler velocimetry was used to obtain real-time measurements of velocity in three flows, the first corresponding to the axisymmetric steady-flow rig of Arcoumanis et al. (1987), the second to the axisymmetric model engine of Arcoumanis et al. (1987) and the third to the modified Citroen engine of Vafidis et al. (1987). The first two flows involved precession of a vortex around an axis of symmetry so that the swirl velocity component provided information of the frequency of the precession and of its radial extent. The third flow, with an off-axis intake valve, was fully three-dimensional and representative of real engines.

The cylinder head for the first two configurations was flat with a single valve located on the axis of symmetry and swirl vanes in the upstream port. In the steady-flow rig, the in-cylinder flow was confined by a porous sintered-bronze plate, located three diameters downstream of the plane of the head, simulating a piston face. In the transparent cylinder model engine, the same cylinder head with a flat piston formed a disc-shaped combustion chamber; the engine was motored at 200 rpm with a compression ratio of 3.5. Futher details of these geometrical arrangements and of the flows within them have been reported by Arcoumanis et al. (1987). The modified Citroen engine was motored at speeds of 1,000 and 1,500 rpm with a compression ratio of 7.5 and the inlet geometry was based on a production engine helical port.

The velocity measurements were obtained with a laser velocimeter operating in the dual-beam, forward-scatter mode and with optical components including an Argon-ion laser operating at 514 nm wavelength and a rotating diffraction grating dividing the incident beam and providing frequency shift. The collecting optics were positioned at an angle to the laser axis in order to minimise the effective size of the measurement volume. The in-cylinder flow was seeded with silicone oil droplets generated in a blast-type atomiser. The forward-scatter arrangement of the laser anemometer and the optical properties of the seeding particles ensured very high data rates in all flow configurations. For example the average data rate in the high speed Citroen engine corresponded to around four valid velocity measurements per degree of crank angle (36 kHz); the corresponding data rate in the low speed model engine was substantially higher. The Doppler signals were processed with a counter (TSI 1990c) interfaced to a computer (IBM/AT compatible) through a DMA card. The individual velocity data and the corresponding crank angle information were stored on hard disk for further processing. All statistics were performed on samples of over 700 cycles, according to the procedures described in the following section.

## 3 Data processing and analysis

Three data processing methods are biefly described below. For the engine data, they consisted of conventional ensemble averaging, high pass filtering (Liou and Santavicca 1983, 1985) and cycle-by-cycle smoothing (Rask 1981). In all cases, all available data were used and no criteria for data rejection were applied.

### *3.1 Ensemble averaging*

The ensemble average mean ($U_{ea}$) and rms ($u_{ea}$) velocities were calculated by arithmetically averaging the instantaneous velocity data in one-degree crank angle intervals over the total number of engine cycles ($N_c = 700-1{,}000$), according to the equations:

$$U_{ea}(\theta) = \frac{1}{N_c} \sum_{i=1}^{N_c} U(\theta, i)$$

$$u_{ea}(\theta) = \left[ \frac{1}{N_c} \sum_{i=1}^{N_c} [U(\theta, i)^2 - U_{ea}(\theta)^2] \right]^{1/2}.$$

### *3.2 High pass filtering*

High pass filtering was performed over the whole range of the same data, (460° or 270°), and in some cases in a smaller window of 120°, centered around top-dead-centre. Each window was split into 512 ($2^9$) intervals and the instantaneous data were averaged to give one velocity value per interval; the Fast Fourier Transform of each cycle trace was then taken. A frequency cut-off was selected by Fourier transforming the ensemble average mean velocity trace and selecting the frequency where this spectrum reached near-zero values ($< 0.2 \times 10^{-4}$). The transforms of the individual cycles were then processed by setting all values of the spectrum above this cut-off frequency to zero and their Inverse Fourier Transform was taken to yield the filtered in-cycle "mean" velocity trace. The filtered rms was computed by subtracting the filtered mean velocity from the corresponding instantaneous velocity and ensemble averaging the result in 1° intervals.

### *3.3 Cycle-by-cycle smoothing*

Cycle-by-cycle smoothing of the velocity data was performed over the 460° window of the model engine measure-

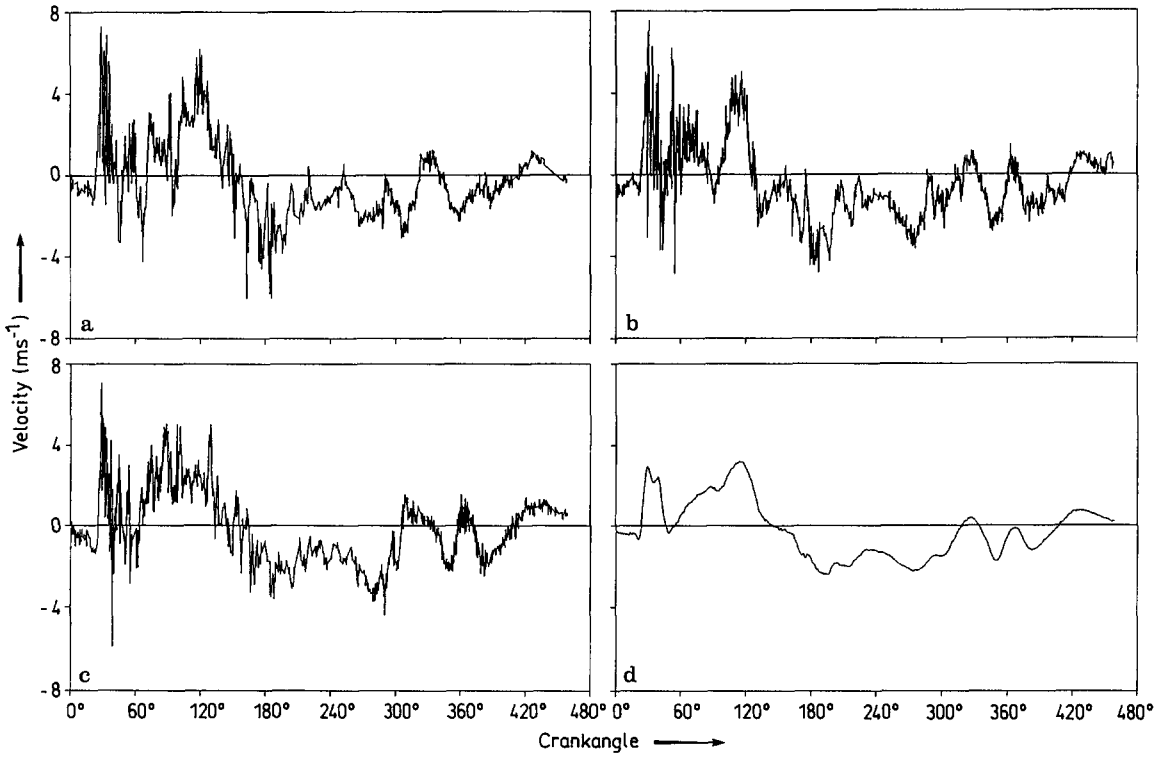


**Fig. 1 a–d.** Variation of the instantaneous (**a–c**) and ensemble-averaged mean (**d**) swirl velocity with crank angle on the centre line of the model engine ($r=0$) at $z=18$ mm

ments only. The instantaneous data were again averaged to give one value per degree and each cycle trace was fitted with a modified cubic spline (Reinsch 1967), using the inverse of the variance as a weighting factor and the number of data plus one (461) as the smoothing factor, (Rask 1981). The resulting smoothed velocity traces were processed as in the high pass filtering method to give mean and rms velocity traces.

The sensitivity of the two cyclic analysis methods was studied by varying the crank angle window, filter setting and smoothing parameter, while the spectra of the velocity fluctuations were obtained by the methods described in the following section.

The steady flow measurements were obtained using the same data acquisition system, but this time the crank angle information was replaced by time information. The data were time-averaged and the corresponding turbulence spectra were obtained using algorithms similar to those of Sect. 3.2 above.

## 4 Results

This section is divided in two parts. The first presents the results of the mean and fluctuating velocity component measurements as obtained in the two engine configurations with the three data processing techniques. The second part deals with the frequency analysis of the same engine data, as well as those of the steady-state analogue, and discusses the implications of the cyclic analysis techniques.

### *4.1 Velocity field measurements*

Figure 1 a–c presents traces of instantaneous swirl velocity obtained on the cylinder axis ($r=0$) of the axisymmetric model engine at $z=18$ mm downstream of the cylinder head. In an ideal situation the ensemble mean velocity should be zero and deviations of the instantaneous traces should be due only to turbulent fluctuations. Instead, they exhibit a periodic oscillation around zero, indicative of swirl centre precession, with larger velocity fluctuations during the induction stroke ($\theta=0-210°$) than during the compression and expansion strokes. There is a definite oscillatory trend of the swirl velocity after inlet valve closure (IVC, $\theta=210°$) which seems to be in phase with the piston motion. The non-random nature of this oscillation is evidenced by the ensemble-averaged mean velocity of 1,000 consecutive cycles (Fig. 1 d) which follows a pattern, similar to that of the instantaneous velocity traces.

Similar data were obtained for both swirl and axial velocity components on the cylinder axis and 20 mm away from it and were processed with the ensemble averaging, high pass filtering and cycle-by-cycle smoothing techniques. The implementation of the high pass filtering technique indicated that the cutoff frequency selection depended on the velocity

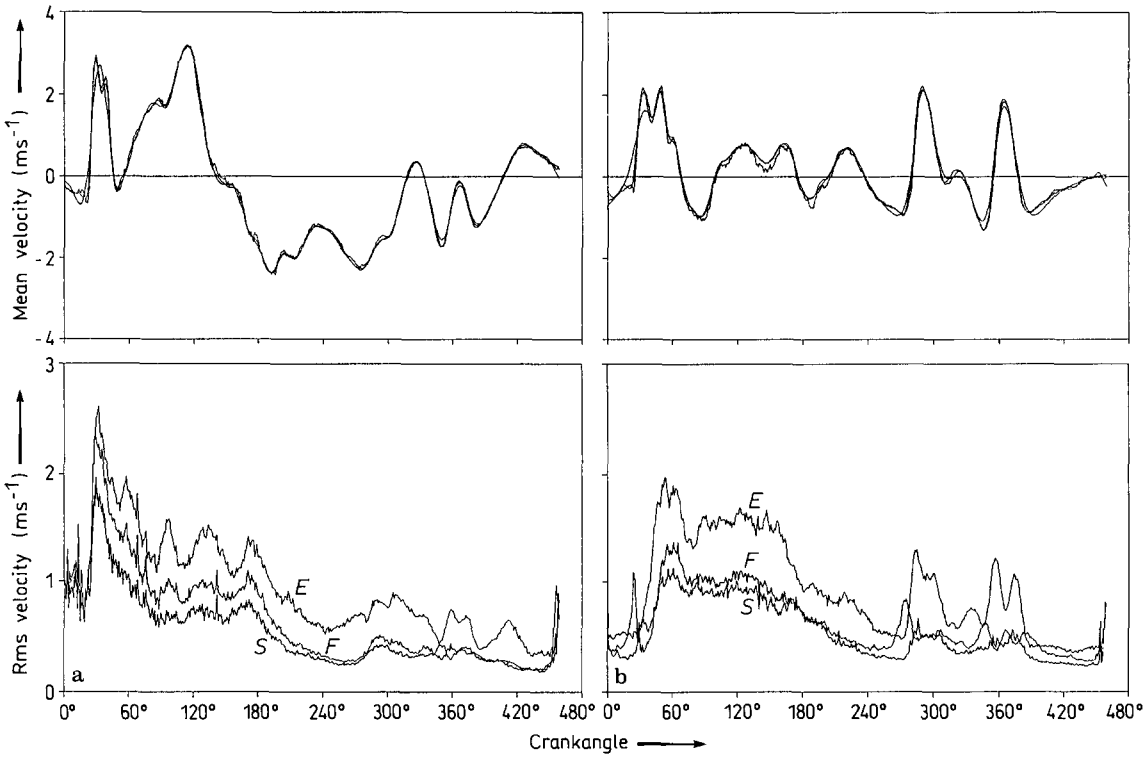


**Fig. 2a and b.** Comparison of the ensemble average (E), high pass filtering (F) and cycle-by-cycle smoothing (S) analysis estimates of the mean and rms of the swirl (**a**) and axial (**b**) velocity fluctuations at $z=18$ and $r=0$ mm in the model engine

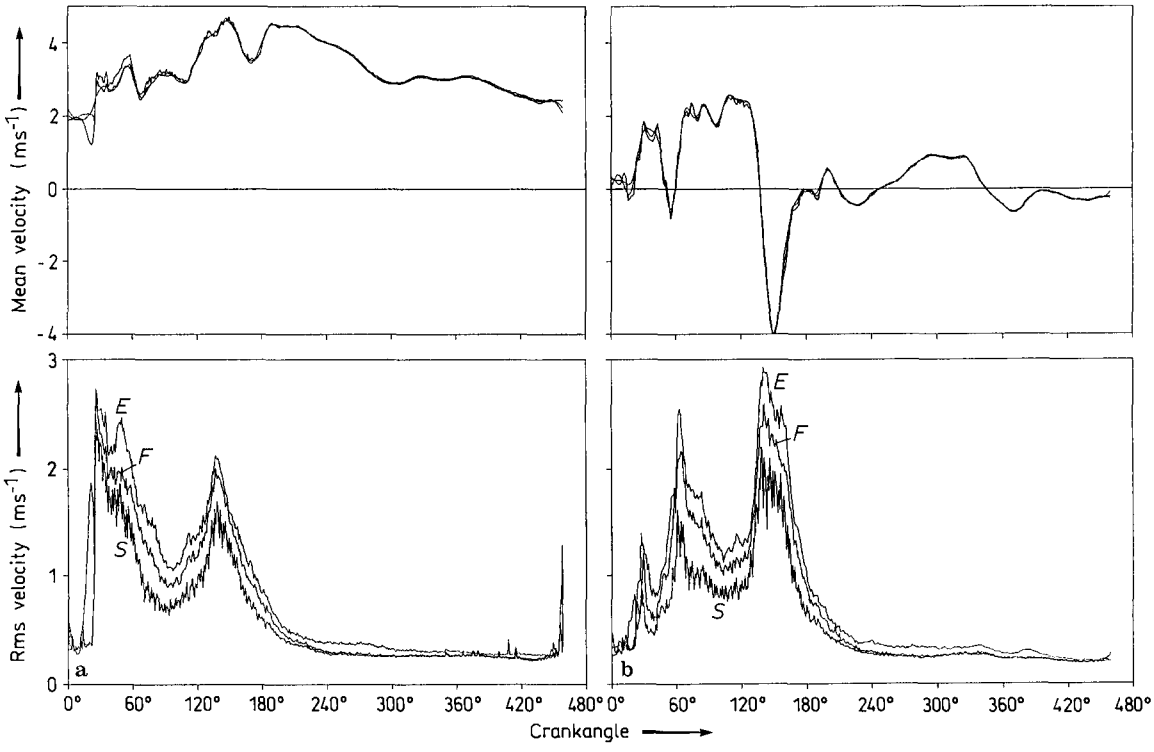


**Fig. 3a and b.** Comparison of the ensemble average (E), high pass filtering (F) and cycle-by-cycle smoothing (S) analysis estimates of the mean and rms of the swirl (**a**) and axial (**b**) velocity fluctuations at $z=18$ and $r=20$ mm in the model engine

component and measurement location. For example, the cutoff frequency for the swirl component on the cylinder axis was determined to be 60 Hz, as opposed to 72 Hz and 92 Hz for the axial component at $r=0$ and 20 mm respectively. Some aspects of the selection of cutoff frequency from the spectrum of the ensemble average mean velocity trace will be discussed below.

The results obtained with the three data analysis methods are shown in Figs. 2 and 3 for the two measurement locations respectively. The swirl and axial mean velocity components on the axis throughout the 460° window show small differences which occur mainly in regions of steep temporal velocity gradients where the high pass filtering method smooths out the higher frequency velocity variations. The results of the cycle-by-cycle smoothing procedure follow the ensemble average mean velocity more closely due to the variable smoothing factor which is determined by the local variance. The rms of the velocity fluctuations in the same window, however, show differences of up to 100% with the ensemble average estimates higher than those of the other two methods, particularly in regions of high temporal velocity gradients. The rms determined by the cycle-by-cycle smoothing procedure is generally lower than that of the filtering method as a result of the closer fit of the individual in-cycle velocity traces obtained with this method. This trend could be reversed by selecting a smoothing parameter other than that proposed by Rask (1981). The results of Fig. 3 show that the differences between the three data processing methods are reduced away from the cylinder axis, with the ensemble average rms estimates being less than 25% higher, particularly after IVC.

The results of the temporal velocity evolution described above, must be considered together with the corresponding spatial distributions. Figure 4 shows the mean and rms of the swirl velocity along the cylinder radius for four selected instances of the 460° window, as evaluated by the ensemble averaging and high pass filtering methods. It can be seen that the differences in the rms estimates increase earlier in the cycle and nearer to the cylinder axis. This, together with the results presented above, leads to the conclusion that the ensemble average rms estimates are broadened by variations of the temporal velocity evolution as well as spatial distribution from one cycle to the next. The effect of these variations is more pronounced in areas of steep temporal and spatial velocity gradients, respectively. It is also clear that the high pass filtering and cycle-by-cycle smoothing techniques minimise this broadening by calculating the rms of the velocity fluctuations on a single-cycle basis, albeit reducing at the same time the overall rms magnitudes by a smaller amount. A question arises, therefore, as to the extent to which low frequency random turbulent fluctuation energy has been removed at the same time as the effects of the ordered cyclic flow variations.

The data of Figs. 2 and 3 were processed using the high pass filtering method in a window of $\pm 60°$ around TDC ($\theta = 300-420°$) as used by Liou and Santavicca (1983, 1985).

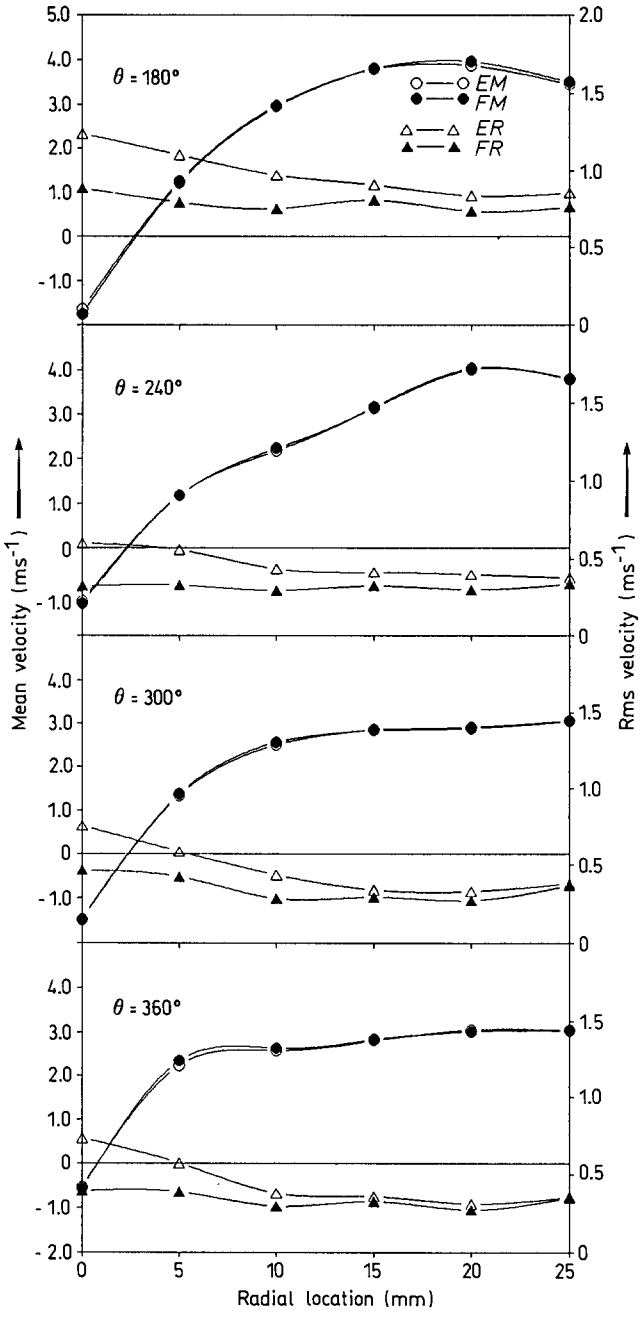


**Fig. 4.** Radial distribution of the ensemble average (o, △) and high pass filtering (●, ▲) analysis estimates of the mean and rms of the swirl velocity fluctuations at various crank angles in the model engine at $z=18$ mm

This may be a better practice since the mean velocity within this interval varies less than in the 460° window and, therefore, the spectral analysis could be more meaningful. The corresponding shortcoming is that the spectral resolution has worsened from 2.6 Hz to 10 Hz as a result of the reduced sampling window. The cutoff frequency defined by the ensemble average mean velocity spectrum for this window was 92 Hz and led to a reduction in rms values of around 20%. A window choice of 204–460° (compression/expan-

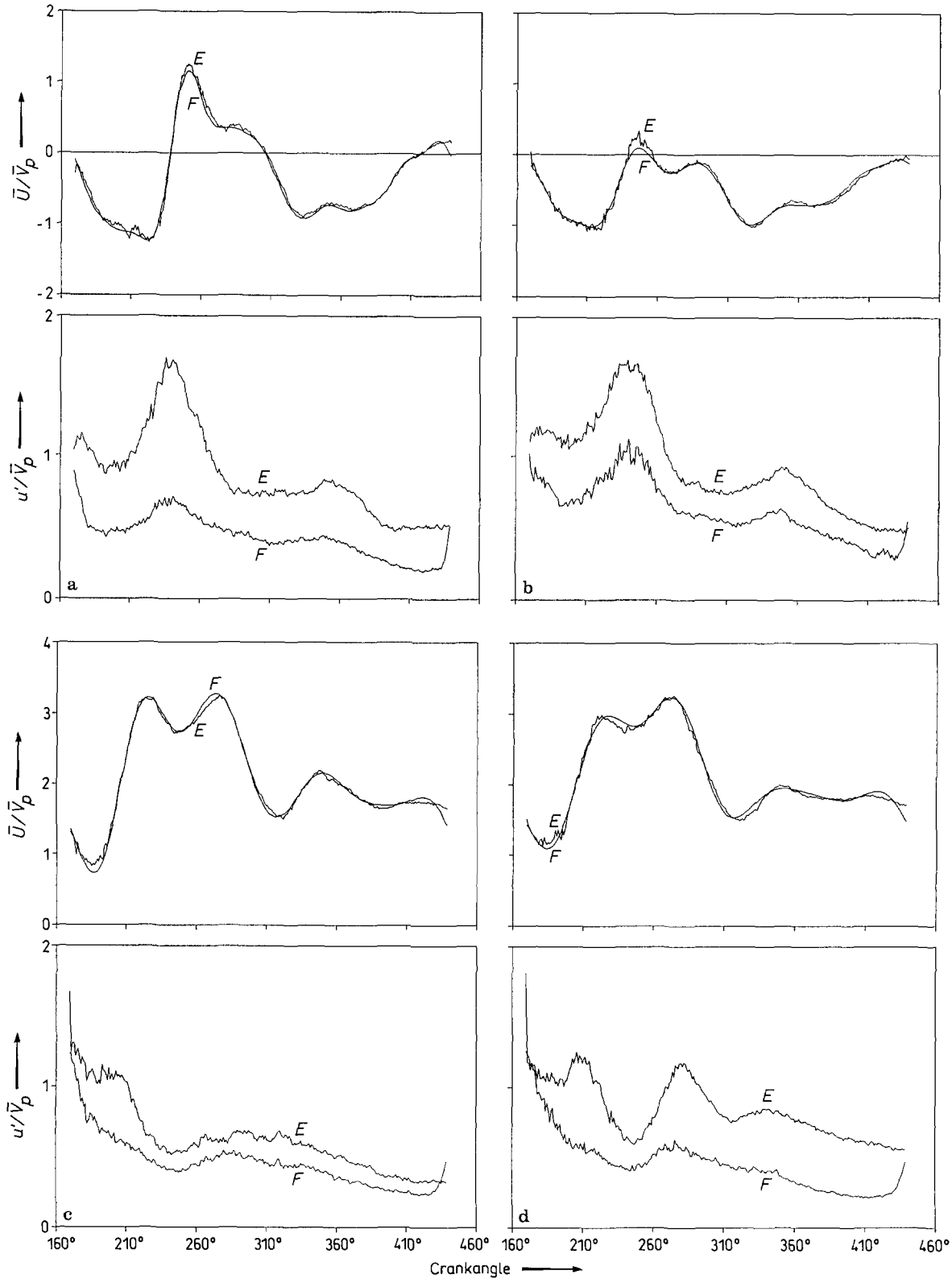


**Fig. 5a–d.** Comparison of the ensemble average (E) and high pass filtering (F) analysis estimates of the mean and rms of the swirl velocity fluctuations at $z = 5.5$ m in the Citroen engine; **a** $r = 0$ mm, 1,000 rpm and **b** 1,500 rpm; **c** $r = 20$ mm, 1,000 rpm and **d** 1,500 rpm

sion strokes) gave a cutoff frequency at 107 Hz and lowered the rms values by a further 5%. This sensitivity of the rms estimates on the selection of frequency cutoff which, in turn, appears to be a function of the selection of sampling window, reduces the credibility of the high pass filtering analysis and raises questions regarding the physical validity of its results.

The effect of engine speed on the frequency cutoff selection was studied in the modified production Citroen 2CV engine, equipped with a helical intake port. The results over a crank angle window of 270°, starting at $\theta = 170°$ ATDC and in the middle of the TDC clearance volume ($z = 5.5$ mm) at radial locations $r = 0$ and 20 mm, are shown in Fig. 5 for speeds of 1,000 rpm (Fig. 5a and c) and 1,500 rpm (Fig. 5b and d). The in-cylinder flow field was not axisymmetric and, although signs of swirl centre precession can be seen near the cylinder axis (Fig. 5a), the cycle-to-cycle repeatability of the swirl velocity oscillatory pattern was poor. This is attributed to the different swirl production mechanism in this engine configuration which also produced a swirl ratio of 3 rather than the 5.5 of the model engine. The associated spatial and temporal swirl velocity gradients were less steep than those observed near the axis of the model engine and led to relatively lower ensemble average rms velocities, despite the lack of cyclic repeatability. Still, the rms velocities near the swirl centre are up to 80% higher than those away from it, suggesting a cyclic variability of the precessing swirl pattern. The cutoff frequencies, determined as in the previous cases, were 245 and 308 Hz for the 1,000 and 1,500 rpm respectively at $r = 0$ mm. Similarly the corresponding cutoff frequencies at $r = 10$ mm were determined as 179 and 201 Hz and at $r = 20$ mm 157 and 200 Hz for the 1,000 and 1,500 rpm respectively and appear to scale (within the frequency resolution of the spectra) with engine speed. The results again illustrate the small differences in the mean velocities evaluated by the ensemble averaging and high pass filtering methods and the large deviations of the rms estimates of the velocity fluctuations which follow trends similar to those observed in the model engine.

### 4.2 *Frequency analysis*

The spectral analysis of transient signals, such as those involved in the implementation of the high pass filtering technique, is subject to uncertainty. The spectral resolution and the FFT algorithm convergence are functions of averaging time which is necessarily short and decreases with decreasing measurement window and increasing engine speed. The upper limit of the frequency spectrum is also defined by the sampling rate which, in the case of in-cylinder measurements, cannot be very high, while the time-varying mean velocity within the sampling window does not allow the application of stationary frequency analysis techniques. Any attempt to reduce the sampling window duration in order to render the velocity signal near-stationary leads to an undesirable decrease of spectral resolution. A more fundamental issue, however, associated with the high pass filtering technique is the discrimination between turbulence and cyclic variations on a time scale basis.

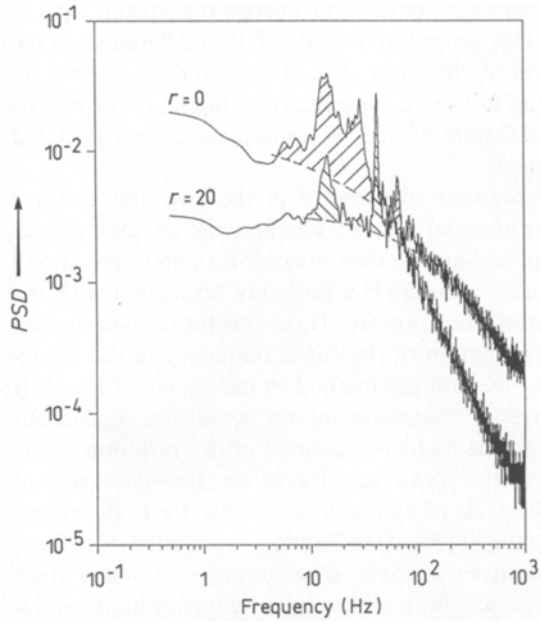


**Fig. 6.** Turbulence spectra of the swirl velocity component at $r = 0$ and 20 mm in the steady-state simulation of the intake stroke; the air volume flow rate corresponds to the mean volume flow rate of the model engine

These considerations led us to examine the in-cylinder velocity spectra as well as those of the corresponding steady-state simulation of the induction stroke. Figure 6 presents the spectra of the swirl velocity fluctuations at locations identical to those considered in the model engine study but obtained with the steady flow arrangement. They correspond to real turbulence spectra with a resolution of 0.5 Hz and extending to 1 kHz. The results show the presence of a distinct peak at 16 Hz at both measurement locations. The frequency at which this PSDF peak occurs was found to vary linearly with volume flow rate and to be directly associated with the precession frequency of the swirl centre (Arcoumanis et al. 1987). The second peak observed around 30–40 Hz is associated with flapping of the annular valve jet (Fansler and French 1988) and is more evident at the measurement location of $r = 20$ mm which is very near to the valve jet shear layer. Both structures are deterministic, may interact and extend over a frequency range between 10 and 50 Hz where considerable turbulent energy exists. The energy below a 60 Hz cutoff frequency at $r = 0$ represents 80% of the total, while at $r = 20$ mm it represents 40%. The high pass filtering at 60 Hz, as suggested by the previous engine data analysis, results in underestimation of the turbulence intensity by 45% at $r = 0$ and by 25% at $r = 20$ mm. Assuming, however, that the contribution of the "deterministic" flow variations is given by the areas immediately under the "humps" of the PSDFs, we can recalculate the turbulence intensity omitting the contribution of the shaded areas

which represent 30% of the total energy at $r=0$ and 14% at $r=20$ mm. This procedure would result in differences in the rms estimates of 20% and 10% at $r=0$ and $r=20$ mm, respectively and is a more conservative estimate of the contribution of the deterministic flow component to the calculated rms magnitudes.

Figure 7 presents the spectra of the ensemble average mean swirl and axial velocity components on the cylinder axis of the model engine over a window of 460° and shows peaks around 20 and 30 Hz, probably associated with the precession of the swirl centre. These spectra have been used for the determination of the cutoff frequency in the implementation of the filtering method in the results of Fig. 2. It should be stressed that these are not turbulence spectra but correspond to the frequency content of the variation of the ensemble average mean velocity within the measurement window. The lack of convergence of the FFT algorithm, evidenced by the ripples of the PSDF, was expected since these spectra come from a single, short duration, velocity trace and makes the definition of the upper frequency limit ambiguous. A further factor to complicate the frequency cutoff selection is the PSDF level to be taken as near-zero. Our convention of PSDF $<0.2\times10^{-4}$ leads to the cutoffs of 60 and 72 Hz for the swirl and axial components respectively but a choice of PSDF $<10^{-5}$ results in cutoffs of more than 100 Hz and a reduction of the filtered rms velocity estimates by more than 20%.

Figure 8 presents the ensemble average mean velocity spectrum over the 460° window of Fig. 7, superimposed on the spectrum of the same velocity trace over the smaller window of 120° around TDC. The spectral resolution has now decreased from 2.6 to 10 Hz and, therefore, the corresponding PSDF appears smoother. It is worth noting that the peak at 30 Hz is now clearly evident, providing further support for the argument that it stems from the precession of the swirl centre. The selection of frequency cutoff is more difficult now since the PSDF values never become much lower than $10^{-4}$. A conservative cutoff selection at 92 Hz (PSD $=2\times10^{-4}$) led to the previously described 20% decrease of the rms estimates.

Since the spectra of the ensemble average mean velocity traces present the convergence difficulties described above, an alternative method could be applied whereby frequency analysis of each of the individual velocity traces is performed and the cutoff frequency is selected from the ensemble average of these spectra in the frequency domain. This technique has been used by Namekawa et al. (1988) but did not eliminate the ambiguity regarding the definition of near-zero PSDF level.

A variant of the above method for processing the instantaneous velocity data was attempted here. The ensemble average mean velocity trace on the cylinder axis was subtracted from each of the instantaneous velocity traces which were then Fourier analysed and the resulting spectra ensemble-averaged in the frequency domain. This method is mathematically valid and corresponds to the trend removal technique, often applied to transient signal analysis, (Bendat and Piersol 1971). The resulting spectra for the two measurement windows of 460° and 120° are shown in Fig. 9 and represent the averaged spectra of the velocity fluctuations around the ensemble average mean, which could be termed turbulence. The results in the 460° window do not show any particular features while those over the 120° window clearly indicate a hump around 30 Hz, similar to those seen in the steady-state turbulence spectrum of Fig. 6. This peak is attributed to the

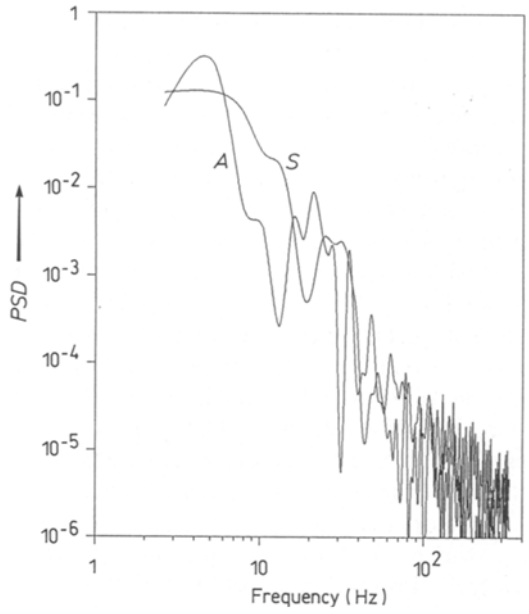


**Fig. 7.** Frequency spectra of the ensemble average mean swirl (S) and axial (A) velocity components at $r=0$ in the model engine over the 460° crank angle window

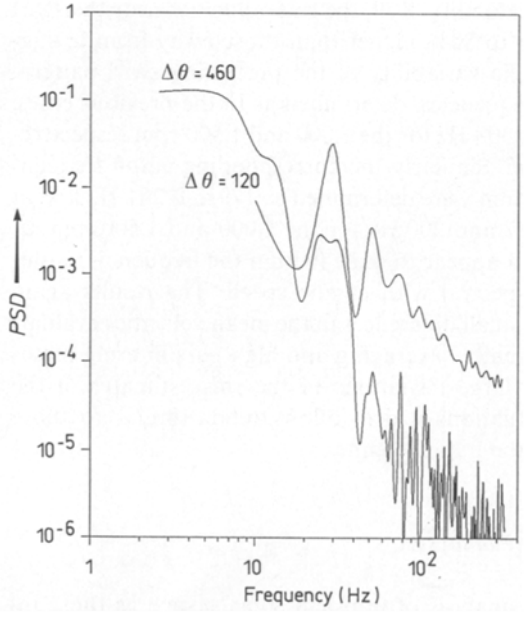


**Fig. 8.** Frequency spectra of the ensemble average mean swirl velocity component at $r=0$ in the model engine over the 460 and 120° crank angle windows

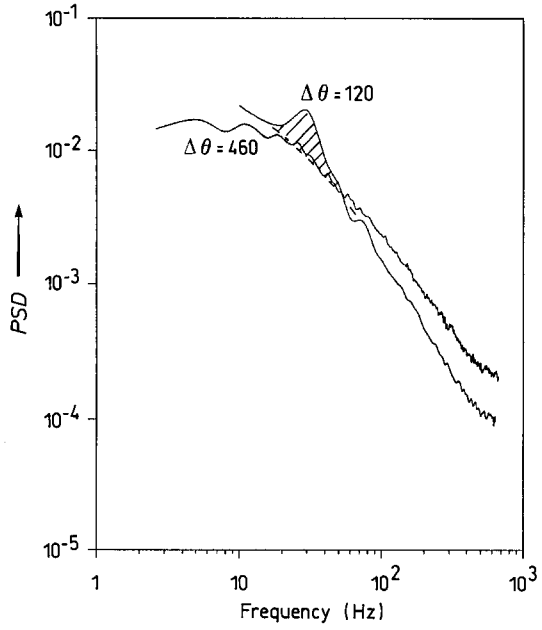


**Fig. 9.** Ensemble average spectra of the swirl velocity fluctuations around the ensemble mean at $r=0$ in the model engine over the 460 and 120° crank angle windows

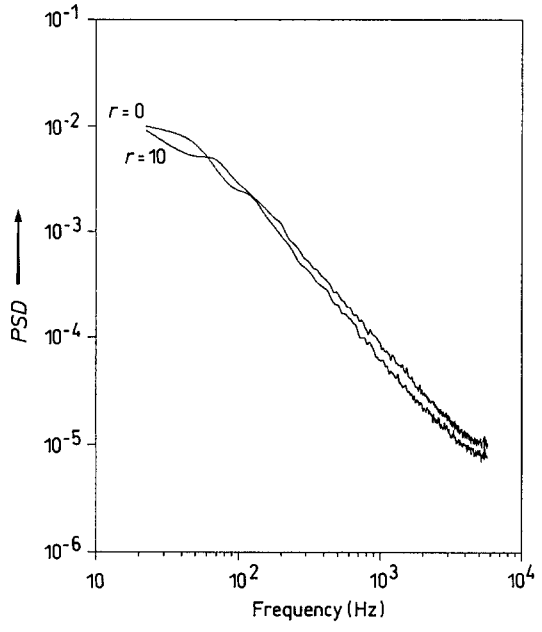


**Fig. 10.** Ensemble average spectra of the swirl velocity fluctuations around the ensemble mean at $r=0$ and $r=10$ mm in the Citroen engine at 1,000 rpm

cyclic phase jitter (Glover 1986) of the precessing swirl vortex and its frequency range is well within that expected to be generated by the variable flow rate during induction. This characteristic frequency range was obviously masked by other contributions over the wider 460° window.

We can treat the spectrum of Fig. 9 in a similar manner to the stationary flow spectra of Fig. 6, although we should bear in mind that the results will reflect averages across the 120° window. The energy associated with the "structured" phenomenon of the swirl centre precession may be given by the area of the hump between 20 and 50 Hz and represents 19% of the total fluctuation energy. Calculation of the rms of the velocity fluctuations, omitting the contribution of the swirl centre precession, will therefore reduce the rms estimate by 10%. If, however, a filter is applied to eliminate all spectral content below 60 Hz, 75% of the total energy will be eliminated leading to 50% lower rms estimates. It can be argued that, in an average over the 120° window, the conventional ensemble averaging overestimates "turbulence" by 10% by including non-stochastic flow variations, while the high pass filtering method underestimates it by 50% by rejecting low frequency turbulent fluctuations. It should be noted that the overestimation of the ensemble averaged rms at specific crank angles can be as high as 100% or as low as 0% depending on the local temporal mean velocity gradient (Fig. 2a).

The ensemble average mean velocity spectra of the Citroen engine data were obtained with a spectral resolution of 22 and 33 Hz for the lower and higher engine speed, respectively, worse than that of the model engine due to the shorter duration of the measurement window and resulted in even more difficult selection of the cutoff frequencies. Contrary to the model engine results, the frequency spectra of the velocity fluctuations around the ensemble mean of the Citroen engine at 1,000 rpm (Fig. 10), did not exhibit any peaks characteristic of ordered motions. This is despite the cyclic variability of the precessing vortex, shown in the previous section, and leads to the conclusion that the frequency characteristics of the swirl centre precession were random and, therefore, not distinguishable from turbulence.

This latter finding raises the question as to whether it is possible to discriminate between turbulence and cyclic flow variations in motored engines. If the cyclic variations are defined as variations of the low frequency (bulk) velocity fluctuations from one cycle to the next, their upper frequency limit is open to arbitrary selection. This is more so if the spectrum of the instantaneous velocity variation in an engine cycle is considered, where no clear separation between low and high frequency fluctuations is present (Liou and Santavicca 1985). It is, therefore, reasonable to expect that by removing the low frequency contributions from the turbulence intensity estimates, part of the turbulent energy is also removed. If, on the other hand, cyclic variability is only attributed to the non-stochastic processes of "cyclic phase or velocity offset" (Glover 1986), their contribution to the rms of the velocity fluctuations can be estimated. Unfortunately, as shown with the Citroen engine results, this is not always the case.

## 5 Concluding remarks

The results of the previous section allow the following conclusions to be drawn:

(1) The mean in-cylinder flow characteristics in a motored reciprocating engine can be determined with simple ensemble averaging or more involved cyclic data analysis techniques with similar results. (2) The application of the high pass filtering technique is subject to uncertainties associated with the spectral analysis of transient signals. (3) High pass filtering of velocity data in order to extract turbulence intensity estimates based on time scale discrimination is subject to arbitrary selection of filtering criteria. It results in underestimation of turbulence magnitudes by removing all energy content below the frequency cutoff. (4) Evaluation of the distribution of fluctuating velocity energy in the frequency domain may reveal the presence of deterministic flow structures, in which case their contribution to the total energy may be estimated and discriminated from that of the random turbulent fluctuations. (5) Large scale velocity variations may not exhibit deterministic characteristics and are, therefore, indistinguishable from turbulence.

## Acknowledgements

The authors are glad to acknowledge support from the EEC, the Joint Research Committee of European Engine Manufacturers, the US Dept. of Energy (Office of Energy Utilisation Research, Energy Conversion and Utilisation Technologies Program) and the Science and Engineering Research Council, U.K.

## References

Arcoumanis, C.; Hadjiapostolou, A.; Whitelaw, J. H. 1987: Swirl center precession in engine flows. SAE Paper 870370

Bendat, S. J.; Piersol, A. G. 1971: Random data: analysis and measurement procedures. New York: Wiley

Catania, A. E.; Mittica, A. 1985: Cycle-by-cycle correlation and spectral analysis of IC engine turbulence. In: Proc. 3rd Int. Symp. on Flows in Internal Combustion Engines, Miami Beach/FL. ASME-FED 28, 39–46

Daily, J. W. 1988: Cycle-to-cycle variations: a chaotic process? Combust. Sci. Technol. 57, 149–162

Fanser, T. D.; French, D. T. 1988: Cycle-resolved laser-velocimetry measurements in a reentrant bowl-in-piston engine. SAE Paper 880377

Glover, A. R. 1986: Towards bias-free estimates of turbulence in engines. 3rd Int. Symp. on Applications of Laser Anemometry to Fluid Mechanics, Lisbon, 5.3

Hall, M. J.; Bracco, F. V.; Santavicca, D. A. 1986: Cycle resolved velocity and turbulence measurements in an IC engine with combustion. SAE Paper 860320

Liou, T.-M.; Santavicca, D. A. 1983: Cycle resolved turbulence measurements in a ported engine with and without swirl. SAE Paper 830419

Liou, T.-M.; Santavicca, D. A. 1985: Cycle resolved LDV measurements in a motored IC engine. J. Fluids Eng. 107, 232–240

Namekawa, S.; Ryu, H.; Asanuma, T. 1988: LDA measurement of turbulent flow in a motored and firing spark-ignition engine with a horizontal prechamber. SAE Paper 881636

Rask, R. B. 1981: Comparison of window, smoothed-ensemble, and cycle-by-cycle data reduction techniques for laser Doppler anemometer measurements of in-cylinder velocity. In: Fluid mechanics of combustion systems (eds. Morel, T.; Lohmann, R. P.; Rackley, J. M.). New York: ASME

Reinsch, C. H. 1967: Smoothing by spline functions. Numer. Math. 10, 177–183

Vafidis, C. 1984: Influence of induction swirl and piston configuration on air flow in a four-stroke model engine. Proc. Inst. Mech. Eng. London 198C. 8, 71–79

Vafidis, C.; Vorropoulos, G.; Whitelaw, J. H. 1987: Effects of intake port and combustion chamber geometry on in-cylinder turbulence in a motored reciprocating engine. In: Proc. Symp. on Fluid Flow and Heat Transfer in Reciprocating Machinery, Boston/MA. ASME-FED 62, 9–15

Winsor, R. E.; Patterson, D. J. 1974: Mixture turbulence – A key to cyclic combustion variation. SAE Paper 730086

Witze, P. O.; Martin, J. K. 1984: Cyclic-variation bias in spark ignition engine turbulence measurements. 2nd Int. Symp. on Applications of Laser Anemometry to Fluid Mechanics, Lisbon, 9.4

Witze, P. O.; Martin, J. K.; Borgnakke, C. 1984: Conditionally-sampled velocity and turbulence measurements in a spark ignition engine. Combust. Sci. Technol. 36, 301

Received February 22, 1990